

Evolutionary dynamics on networks of selectively neutral genotypes: Effects of topology and sequence stability

Jacobo Aguirre,¹ Javier M. Buldú,² and Susanna C. Manrubia¹

¹*Centro de Astrobiología, CSIC-INTA, Ctra. de Ajalvir km 4, 28850 Torrejón de Ardoz, Madrid, Spain*

²*Complex Systems Group, Signal Theory and Communications Department, U.R.J.C., Camino del Molino s/n, 28943, Fuenlabrada, Madrid, Spain*

(Received 17 July 2009; published 14 December 2009)

Networks of selectively neutral genotypes underlie the evolution of populations of replicators in constant environments. Previous theoretical analysis predicted that such populations will evolve toward highly connected regions of the genome space. We first study the evolution of populations of replicators on simple networks and quantify how the transient time to equilibrium depends on the initial distribution of sequences on the neutral network, on the topological properties of the latter, and on the mutation rate. Second, network neutrality is broken through the introduction of an energy for each sequence. This allows to study the competition between two features (neutrality and energetic stability) relevant for survival and subjected to different selective pressures. In cases where the two features are negatively correlated, the population experiences sudden migrations in the genome space for values of the relevant parameters that we calculate. The numerical study of larger networks indicates that the qualitative behavior to be expected in more realistic cases is already seen in representative examples of small networks.

DOI: [10.1103/PhysRevE.80.066112](https://doi.org/10.1103/PhysRevE.80.066112)

PACS number(s): 89.75.Hc, 87.23.Kg, 87.10.-e

I. INTRODUCTION

One of the tenets of the Darwinian theory of evolution is that the fittest variants in a population increase in number and might eventually get fixed, thus eliminating less fit forms. Fitness refers to the phenotype of individuals, to the measurable features that determine their suitability in a given environment. The phenotype is the target of selection, but random mutations, responsible for the generation of new variants, can only act on the genotype. A better comprehension of the complex map between genotype and phenotype is an essential issue in the effort to understand the mechanisms behind evolution and adaptation of populations, among others their robustness in the face of perturbations or the appearance of novelty.

There is abundant evidence of the existence of an extremely large degeneration between genotype and phenotype. In other words, the same phenotype can be obtained from a huge number of different genotypes. This ensemble forms the *neutral network* of genotypes corresponding to a given phenotype. The idea of neutral evolution was first introduced by Kimura [1] in order to account for the known fact that a large number of mutations observed in proteins, DNA, or RNA, did not have any effect on fitness.

RNA sequences folding into their minimum free-energy secondary structures are likely the most used model of the genotype-phenotype relationship [2–4]. Analytical studies of the number of sequences of length l compatible with a fixed secondary structure (used as a proxy for the phenotype) have revealed that the average size of the corresponding neutral network grows as $l^{3/2}b^l$, where b is a constant [5]. Hence, there should be about 10^{28} sequences compatible with the structure of a transfer RNA (which has length $l=76$), while the currently known smallest functional RNAs, of length $l \approx 14$ [6], could in principle be obtained from more than 10^6 different sequences. Neutral networks are astronomically

large even for moderate values of the sequence length.

Neutrality becomes particularly important in the evolution of quasispecies [7], populations of fast mutating replicators which are formed by a large number of different phenotypes—and many more genotypes—, and where high diversity and the concomitant steady exploration of the genome space happen to be an adaptive strategy. Relevant examples of quasispecies of RNA molecules are RNA viruses [8] and error-prone replicators in the context of the RNA world [9]. Evolutionary innovation in quasispecies is facilitated by the fact that most neutral networks span the whole space of genomes. Actually, taking again the case of the RNA sequence-structure map as example, all common structures of length l can be found within a relatively small radius (measured as the number of nucleotides that have to be changed) of a randomly chosen sequence in genotype space [10], thus showing that neutral networks are deeply interwoven. The mutual proximity of neutral networks in genome space has received empirical support from studies showing how two sequences differing in only two nucleotides can fold and function as fully different ribozymes [11] and how diffusion on neutral networks promotes innovation in the evolution of influenza A [12]. Diffusion through neutral networks is thus regarded as an essential component of the adaptation of quasispecies to changing environments, which demand new functional phenotypes to guarantee survival.

In the absence of environmental changes, quasispecies stay on the same neutral network and evolve toward regions denser in neutral genotypes. In these regions, the probability that upon replication a random mutation produces a sequence with a different fold is minimized, such that mutational robustness is maximized. Models of evolution on neutral networks use to define genotypes as the nodes of the network; two nodes are linked when their sequences are at a Hamming distance of one, that is, when they differ in only one nucleotide [13,14]. In this scenario, and when the dynamics are

dominated by selection, the equilibrium state of the population only depends on the topology of the neutral network [15,16]. However, the final state might depend as well on the mutation rate when random drift becomes an important component of the dynamics [17,18] or when links that extend beyond nearest-neighbor sequences are considered [19].

Despite the expected advantage that more neutral variants should occasionally have in competition with fitter but less robust types [20], selection of highly neutral genotypes has been observed in very few natural cases [21,22]. This partly negative result admits different explanations. Among others, it might be that high neutrality hinders evolvability [23] or critically delays the recovery of the population after strong reductions in its size [24]. In presence of stronger selection of other phenotypic traits there might be tradeoffs that forbid the simultaneous optimization of both of them. Finally, a given environment should keep constant for a long enough time as to allow the selection of highly neutral genotypes: if the environment changes in time scales typically shorter than those allowing the selection of high neutrality, the latter will not be observed.

The scenario thus far described acts as motivation to undertake the present study. In this work we address the evolution of populations of replicators on artificial neutral networks with two goals in mind. First, we quantify the transient time before equilibrium is reached and relate it to the topological properties of the neutral network, with the initial distribution of sequences on it, and with the mutation rate. Second, we study the evolution of the population on small networks where neutrality is broken by assigning an energy to each node. In a final study of large, complex networks, nodes are explicitly represented by sequences, such that their energy is a function of the composition of a sequence, as is known to occur in real cases [25,26]. The use of two phenotypic characteristics, neutrality and energy, allows then to mimic the competition between two different features subjected to different selective pressures. The relative intensity of selection is tuned through an appropriate selection parameter. The examples we use in this study might not correspond to any natural neutral network, but our results indicate that they are able to capture the qualitative behavior to be expected in more realistic cases. In particular, although a neutral network can in principle be formed by an arbitrary number of disconnected components (depending on sequence length and the secondary structure chosen), we restrict our investigation to the evolution on a single connected component of the total network.

The paper is organized as follows. In Sec. II we introduce the specific dynamical system used and present general analytical results regarding evolution of an infinite population on an arbitrary neutral network. In particular, we prove that the time to equilibrium is inversely proportional to the mutation rate. In Sec. III we assign an energy to each of the nodes of our networks and present the dynamical equations and some general analytical results when neutrality and stability are simultaneously under selection. In Sec. IV we discuss representative examples of small networks when neutrality and stability are positively and negatively correlated. Of special interest is the case of a four-node network where the sequence of minimal folding energy is that with the low-

est connectivity. This causes a nonmonotonic behavior of the time to equilibrium with the selection parameter and sudden transitions in the localization of the equilibrium states. Small networks settle the bases to comprehend the phenomenology observed in larger, more realistic networks with different topologies investigated in Sec. V. We conclude with our main results and an overall discussion in Sec. VI.

II. NEUTRAL NETWORKS OF IDENTICAL NODES

In this section we study the dynamics of a population of individuals on a network where all nodes (sequences) have the same selective value. The network is thus completely specified through the adjacency matrix \mathbf{C} of the corresponding undirected, connected graph. Sequences replicate and daughter sequences have a probability to mutate. The actual dynamics of sequences are implemented in an effective fashion, as will be shown. The results presented in Secs. II A and II B 1 are known. They were reported in previous works [15,16] and are here rephrased in the framework of our dynamical equations for completeness.

A. Definitions and dynamical equations

Each node i in the network holds a number $n_i(t)$ of sequences at time t . There are $i=1, \dots, m$ nodes in the network, each with a degree (number of nearest neighbors) k_i . The total population will be maintained constant through evolution, $N=\sum_i n_i(t)$, and we assume $N \rightarrow \infty$ to avoid stochastic effects due to finite population sizes. The initial distribution of sequences on the network at $t=0$ is $n_i(0)$. Sequences of length l formed by 4 different nucleotides have at most $3l$ neighbors. We call $\{nm\}_i$ the set of actual neighbors of node i , whose cardinal is k_i . The vector \vec{k} has as components the degree of the $i=1, \dots, m$ nodes of the network. At each time step, the sequences at each node replicate. Daughter sequences mutate to one of the $3l$ nearest neighbors with probability μ , and remain equal to their mother sequence with probability $1-\mu$. In our representation $0 < \mu \leq 1$. The singular case $\mu=0$ is excluded to avoid trivial dynamics and guarantee evolution toward a unique equilibrium state. With probability $k_i/(3l)$, the mutated sequence exists in the neutral network and it adds to the population of the corresponding neighboring node. Otherwise, it falls off the network and disappears, this being the fate of a fraction $[1-k_i/(3l)]\mu$ of the total daughter sequences. Note that, in this effective representation, l simply controls the dilution of the network and thus the relative fraction of viable vs nonviable mutants generated upon replication.

The mean-field equations describing the dynamics of the population on the network read

$$n_i(t+1) = (2-\mu)n_i(t) + \frac{\mu}{3l} \sum_{j \in \{nm\}_i} n_j(t). \quad (1)$$

The dynamics can be written in matrix form as

$$\vec{n}(t+1) = (2-\mu)\mathbf{I}\vec{n}(t) + \frac{\mu}{3l}\mathbf{C}\vec{n}(t), \quad (2)$$

where \mathbf{I} is the identity matrix and \mathbf{C} is the adjacency matrix of the network, whose elements are $C_{ij}=1$ if nodes i and j

are connected and $C_{ij}=0$ otherwise. The transition matrix \mathbf{M} is defined as

$$\mathbf{M} = (2 - \mu)\mathbf{I} + \frac{\mu}{3l}\mathbf{C}. \quad (3)$$

Let us call $\{\lambda_i\}$ the set of eigenvalues of \mathbf{M} , with $\lambda_i \geq \lambda_{i+1}$, and $\{\vec{u}_i\}$ the corresponding eigenvectors. The spectral theorem states that, as \mathbf{M} is real and symmetric, it admits the decomposition

$$\mathbf{M} = \mathbf{P}\mathbf{G}\mathbf{P}^{-1} = \mathbf{P}\mathbf{G}\mathbf{P}^T, \quad (4)$$

where \mathbf{P} has the eigenvectors of \mathbf{M} as columns and \mathbf{G} is a real diagonal matrix with the eigenvalues of \mathbf{M} ordered along the diagonal. Furthermore, its eigenvectors verify $\vec{u}_i \cdot \vec{u}_j = 0$, $\forall i \neq j$ and $|\vec{u}_i| = 1$, $\forall i$.

Since \mathbf{M} is a primitive matrix [39], the Perron-Frobenius theorem assures that, in the interval of μ values used, the largest eigenvalue of \mathbf{M} is positive, $\lambda_1 > |\lambda_i|$, $\forall i > 1$, and its associated eigenvector is positive (i.e., $(\vec{u}_1)_i > 0$, $\forall i$).

The dynamics of the system, Eq. (2) can be thus written as

$$\vec{n}(t) = \mathbf{M}^t \vec{n}(0) = \sum_{i=1}^m \lambda_i^t \alpha_i \vec{u}_i, \quad (5)$$

where we have defined α_i as the projection of the initial condition on the i th eigenvector of \mathbf{M} ,

$$\alpha_i = \vec{n}(0) \cdot \vec{u}_i. \quad (6)$$

Furthermore, as $\lambda_1 > |\lambda_i|$, $\forall i > 1$, the asymptotic state of the population is proportional to the eigenvector that corresponds to the largest eigenvalue, \vec{u}_1 ,

$$\lim_{t \rightarrow \infty} \left(\frac{\vec{n}(t)}{\lambda_1^t \alpha_1} \right) = \vec{u}_1, \quad (7)$$

while the largest eigenvalue λ_1 yields the growth rate of the population at equilibrium (in the absence of rescaling). For convenience, in the following, and without any loss of generality, we normalize the population $\vec{n}(t)$ such that $|\vec{n}(t)| = 1$ after each generation. With this normalization, $\vec{n}(t) \rightarrow \vec{u}_1$ when $t \rightarrow \infty$.

B. Results

1. Network topology and asymptotic states

Let us call $\{\gamma_i\}$ the set of eigenvalues of matrix \mathbf{C} , $\gamma_i \geq \gamma_{i+1}$, and $\{\vec{w}_i\}$ the set of corresponding eigenvectors. From Eq. (3),

$$\mathbf{M}\vec{w}_i = (2 - \mu)\mathbf{I}\vec{w}_i + \frac{\mu}{3l}\mathbf{C}\vec{w}_i = \left[(2 - \mu) + \frac{\mu}{3l}\gamma_i \right] \vec{w}_i. \quad (8)$$

The eigenvectors of the adjacency matrix are also eigenvectors of the transition matrix, $\vec{u}_i \equiv \vec{w}_i$, $\forall i$, demonstrating that the asymptotic state of the population only depends on the topology of the neutral network. The eigenvalues of both matrices are thus related through

$$\lambda_i = (2 - \mu) + \frac{\mu}{3l}\gamma_i, \quad (9)$$

where the set $\{\gamma_i\}$ does not depend on the mutation rate μ . The adjacency matrix contains all the information on the final states, while the transition matrix yields quantitative information on the dynamics toward equilibrium.

The minimal value of λ_1 is obtained in the limit of a population evolving at a very high mutation rate ($\mu \rightarrow 1$) on an extremely diluted matrix ($l \rightarrow \infty$). In this limit, all eigenvalues of \mathbf{M} become asymptotically independent of the precise topology of the network and $\lambda_i \rightarrow 1$, $\forall i$. In this extreme case all daughter sequences fall off the network, but the population is maintained constant through the parental population. An extinction catastrophe (due to a net population growth below one [30]) never holds under this dynamics.

The *average degree* $K(t)$ of the population at time t is defined as

$$K(t) = \frac{\vec{k} \cdot \vec{n}(t)}{\sum_i n_i(t)}. \quad (10)$$

In the limit $t \rightarrow \infty$, we obtain the average degree at equilibrium

$$K(t \rightarrow \infty) = K = \frac{\vec{k} \cdot \vec{u}_1}{\sum_i (u_1)_i}. \quad (11)$$

We define as k_{min} , k_{max} , and $\langle k \rangle = \sum_i k_i / m$ the smallest, largest, and average degree of the network, respectively. The Perron-Frobenius theorem for non-negative, symmetric, and connected graphs, sets limits on the average degree $\langle k \rangle$: when $k_{min} < k_{max}$, that is, as far as the graph is not homogeneous,

$$k_{min} < \langle k \rangle < k_{max} \quad (12)$$

holds. A simple calculation (based on the identity between the eigenvectors of the adjacency matrix \mathbf{C} and the transition matrix \mathbf{M}) yields that the average degree of the population at equilibrium, K , is equal to the largest eigenvalue γ_1 of the adjacency matrix, also known as the spectral radius of the network [15]. Therefore, from Eq. (12) we obtain that the average degree K of the population at equilibrium will be larger than the average degree $\langle k \rangle$ of the network, indicating that when all nodes are identical the population selects regions with connectivity above average.

2. Dynamics toward equilibrium

Equation (5) describes the transient dynamics toward equilibrium starting with an initial condition $\vec{n}(0)$. The distance $\Delta(t)$ to the equilibrium state can be written as

$$\Delta(t) \equiv \left| \frac{\mathbf{M}^t \vec{n}(0)}{\lambda_1^t \alpha_1} - \vec{u}_1 \right| = \left| \sum_{i=2}^m \vec{\Delta}_i(t) \right| = \left| \sum_{i=2}^m \frac{\alpha_i}{\alpha_1} \left(\frac{\lambda_i}{\lambda_1} \right)^t \vec{u}_i \right|. \quad (13)$$

In order to estimate how many generations elapse before

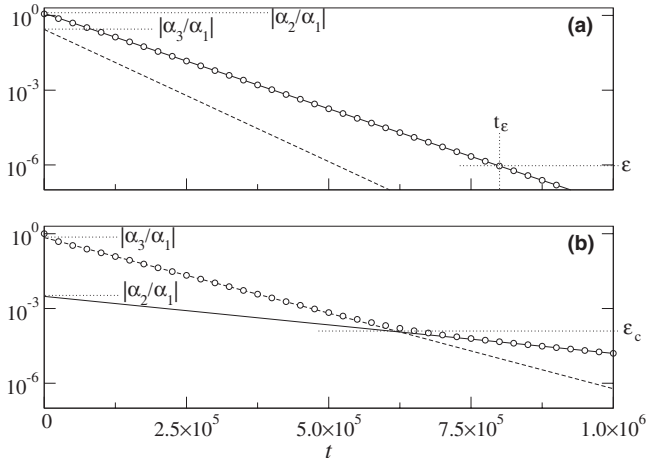


FIG. 1. Sketch of the evolution with time of the distance to the equilibrium state $\Delta(t)$ (\circ), $|\overline{\Delta}_2(t)|$ (solid line) and $|\overline{\Delta}_3(t)|$ (dashed line). Two different cases are plotted: (a) If $|\alpha_2| > |\alpha_3|$, then $\Delta(t) \approx |\overline{\Delta}_2(t)|$, $\forall t$ and Eq. (14) is valid $\forall \epsilon$. (b) When $|\alpha_3| \gg |\alpha_2|$ and $|\lambda_3| \approx |\lambda_2|$, t_ϵ^1 yields an accurate estimation of t_ϵ if $\epsilon < \epsilon_c$.

equilibrium is reached, we fix a threshold ϵ , and define the *time to equilibrium* t_ϵ as the number of generations required for $\Delta(t_\epsilon) < \epsilon$.

When $\alpha_2 \neq 0$, $\lambda_2 \neq 0$, and $\lambda_2 \neq \lambda_3$, t_ϵ can be approximated to first order by

$$t_\epsilon^1 \approx \frac{\ln|\alpha_2/\alpha_1| - \ln \epsilon}{\ln|\lambda_1/\lambda_2|}. \quad (14)$$

This approximation turns out to be extremely good in most cases thanks to the exponentially fast suppression of the contributions due to higher-order terms (since $\lambda_i \geq \lambda_{i+1}$, $\forall i$). It may lose accuracy, however, when $\lambda_3 \approx \lambda_2$, when the initial condition $\vec{n}(0)$ is such that $|\alpha_3| \gg |\alpha_2|$, or when ϵ is so large that the population is far from equilibrium and $\Delta(t)$ is still governed by λ_3 and higher-order eigenvalues.

Formally, Eq. (14) will accurately estimate t_ϵ if $|\overline{\Delta}_3(t)| < |\overline{\Delta}_2(t)|$ in the development of Eq. (13),

$$\left| \frac{\alpha_2}{\alpha_1} \right| \left| \frac{\lambda_2}{\lambda_1} \right|^{t_\epsilon} > \left| \frac{\alpha_3}{\alpha_1} \right| \left| \frac{\lambda_3}{\lambda_1} \right|^{t_\epsilon}. \quad (15)$$

For arbitrary topologies and initial conditions, the previous inequality implicitly defines a value ϵ_c below which it always holds. Using Eq. (14) to approximate the value of t_ϵ , we can estimate in a self-consistent fashion that, $\forall \epsilon$ fulfilling

$$\epsilon < \epsilon_c = \left| \frac{\alpha_2}{\alpha_1} \right| \exp \left(- \frac{\log \left| \frac{\alpha_3}{\alpha_2} \right| \log \left| \frac{\lambda_1}{\lambda_2} \right|}{\log \left| \frac{\lambda_2}{\lambda_3} \right|} \right) \quad (16)$$

the time t_ϵ^1 , as explicitly obtained from Eq. (14), accurately approximates t_ϵ , as implicitly defined by Eq. (13). Examples of different situations are shown in Fig. 1, showing that t_ϵ^1 is generically a good approximation when a sufficiently small distance ϵ to equilibrium is required.

The functional relationship between the time to equilibrium and the mutation rate can be obtained by developing Eq. (14) in powers of μ ,

$$t_\epsilon^1 = \ln \left(\left| \frac{\alpha_2}{\epsilon \alpha_1} \right| \right) \left[\frac{a}{\mu} + b - c\mu \right] + O(\mu^2), \quad (17)$$

where

$$a = \frac{6l}{(\gamma_1 - \gamma_2)}, \quad b = \frac{\gamma_1 + \gamma_2 - 6l}{2(\gamma_1 - \gamma_2)}, \quad c = \frac{\gamma_1 - \gamma_2}{72l}. \quad (18)$$

Since $c \ll a$, the dependence of the time to equilibrium with the mutation rate follows $t_\epsilon^1 \propto \mu^{-1}$, and therefore μ sets the rate at which equilibrium is approached, for a fixed topology of the neutral network. Finally, changes in the adjacency matrix also affect how fast equilibrium can be reached, through the values of γ_1 and γ_2 .

3. Exactly solvable examples

Consider a star formed by m nodes, 1 in the center with connectivity $m-1$ and $m-1$ nodes in the periphery with connectivity 1. The adjacency matrix has eigenvalues $\{\gamma_i\} = \{\sqrt{m-1}, 0, 0, 0, \dots, 0, 0, -\sqrt{m-1}\}$. This implies that the eigenvalues of the transition matrix for this case read

$$\lambda_1 = (2 - \mu) + \frac{\mu}{3l} \sqrt{m-1},$$

$$\lambda_i = (2 - \mu), \quad 2 \leq i \leq m-1,$$

$$\lambda_m = (2 - \mu) - \frac{\mu}{3l} \sqrt{m-1}. \quad (19)$$

The eigenvectors for both matrices are $\vec{u}_1 = (2m-2)^{-1/2}(\sqrt{m-1}, 1, 1, 1, \dots, 1, 1)$, $\vec{u}_m = (2m-2)^{-1/2}(-\sqrt{m-1}, 1, 1, 1, \dots, 1, 1)$, and $\vec{u}_i = 2^{-1/2}(0, -1, 0, 0, \dots, 0, 1, 0, 0, \dots, 0)$, where 1 is at the position $i+1$, for $2 \leq i \leq m-1$.

Let us consider the initial condition $\vec{n}(0) = N^{-1/2}(1, 1, 1, \dots, 1, 1)$. The values of the coefficients α_i become

$$\alpha_1 = \vec{u}_1 \cdot \vec{n}(0) = \frac{1}{\sqrt{2N}}(1 + \sqrt{m-1}),$$

$$\alpha_i = \vec{u}_i \cdot \vec{n}(0) = 0, \quad 2 \leq i \leq m-1,$$

$$\alpha_m = \vec{u}_m \cdot \vec{n}(0) = \frac{1}{\sqrt{2N}}(-1 + \sqrt{m-1}). \quad (20)$$

This case is interesting because, for an homogeneously distributed initial population, the distance to equilibrium is dominated by the smallest eigenvalue. According to Eq. (13), we obtain the exact result

$$\Delta(t) = \frac{-1 + \sqrt{m-1}}{1 + \sqrt{m-1}} \left(\frac{(2 - \mu) - \mu/(3l)\sqrt{m-1}}{(2 - \mu) + \mu/(3l)\sqrt{m-1}} \right)^t, \quad (21)$$

from where the exact time to equilibrium can be explicitly obtained, once the threshold distance $\Delta(t) < \epsilon$ is fixed. If we

develop the time to equilibrium in powers of the number of nodes m and the mutation rate μ , we obtain $t_\epsilon \propto \mu^{-1}$ [in agreement with the generic dependence derived in Eq. (17)], and $t_\epsilon \propto m^{-1/2}$. This latter result depends on the topology of \mathbf{C} and thus is not generic.

Take as a second example the case of a completely connected network, where $C_{ij}=1, \forall i \neq j$. Now $\gamma_1=m-1, \gamma_i=-1, \forall i>1, \vec{u}_1=m^{-1/2}(1,1,\dots,1,1)$, and $\vec{u}_i=2^{-1/2}(-1,0,\dots,0,1,0,\dots,0)$, where 1 is at the position i , for $(2 \leq i \leq m)$. Repeating the development above, we can also obtain the exact expressions for the distance to equilibrium $\Delta(t)$ and the time to equilibrium t_ϵ . In this case, the initial condition will be $\vec{n}(0)=(1,0,0,\dots,0)$ [40], which implies $\alpha_1=\frac{1}{\sqrt{m}}$ and $\alpha_i=-\frac{1}{\sqrt{2}}, \forall i>1$. The distance to equilibrium becomes

$$\Delta(t) = \left| \frac{\alpha_2}{\alpha_1} \right| \left| \frac{\lambda_2}{\lambda_1} \right| \left| \sum_{i=2}^m \vec{u}_i \right|, \quad (22)$$

$$= \frac{m\sqrt{m-1}}{2} \left| \frac{(2-\mu) - \mu/(3l)}{(2-\mu) + \mu/(3l)(m-1)} \right|^t. \quad (23)$$

As previously, we develop the time to equilibrium t_ϵ in powers of the mutation rate μ to obtain $t_\epsilon \propto \mu^{-1}$. When developing it in powers of the number of nodes m , we obtain that t_ϵ depends on m in a functionally complex manner, but, asymptotically, $t_\epsilon \rightarrow 3/2$ when $m \rightarrow \infty, \forall \mu, \epsilon, l$.

III. NEUTRAL NETWORKS OF DISTINGUISHABLE NODES

Genotypes are not identical from a strict point of view, be it only because their sequences are different. Changes in sequence composition may affect the processivity of a genome, the strength of interaction with other molecules or, in the case we are considering, the energy of the folded state. In this section, we label each node with an additional parameter E_i which can be understood as a measure of the thermodynamical stability of the corresponding sequence. To begin with, we do not constrain the range of values of E_i and do not relate it with any other property of the node.

We will define the probability p_i that a sequence stays at a particular node as a function of its energy: the higher E_i , the lower the probability of occupation of node i ,

$$p_i = \exp\{-\beta(E_i - E_{min})\}, \quad (24)$$

where the minimum energy in the network E_{min} serves to normalize the probability, $0 < p_i \leq 1$. The selection parameter β quantifies the intensity of selection for energy versus selection for neutrality. In the limit $\beta \rightarrow 0$ one recovers the results of the case where nodes are identical, while in the limit $\beta \rightarrow \infty$ we expect the population to concentrate at the nodes with minimum energy.

A. Dynamical equations

With the introduction of selection for energy, the dynamical equations become

$$n_i(t+1) = \left[(2-\mu)n_i(t) + \frac{\mu}{3l} \sum_{\{nm\}_i} n_j(t) \right] e^{-\beta(E_i - E_{min})}, \quad (25)$$

and in matrix form

$$\vec{n}(t+1) = \left[(2-\mu)\mathbf{E}\mathbf{I} + \frac{\mu}{3l}\mathbf{E}\mathbf{C} \right] \vec{n}(t). \quad (26)$$

The transition matrix reads

$$\mathbf{M}' = \mathbf{E} \left[(2-\mu)\mathbf{I} + \frac{\mu}{3l}\mathbf{C} \right] = \mathbf{E}\mathbf{M}, \quad (27)$$

where \mathbf{E} is a diagonal matrix with elements $E_{ij} = e^{-\beta(E_i - E_{min})} \delta_{ij}$, and \mathbf{M} is the transition matrix for the case of identical nodes. Let us call $\{\lambda_i\}$ the set of eigenvalues of \mathbf{M}' , with $\lambda_i \geq \lambda_{i+1}$, and $\{\vec{u}_i\}$ and $\{\vec{u}_i^L\}$ its corresponding sets of right and left eigenvectors. The matrix \mathbf{M}' is not symmetric, but it is symmetrizable, thus admitting the decomposition

$$\mathbf{M}' = \mathbf{Q}\mathbf{H}\mathbf{Q}^{-1}, \quad (28)$$

where \mathbf{H} is a diagonal matrix [41].

As \mathbf{M}' is not symmetric, its left and right eigenvectors do not coincide: \mathbf{Q} has the right eigenvectors of \mathbf{M}' as columns, \mathbf{Q}^{-1} has the left eigenvectors of \mathbf{M}' as rows, and \mathbf{H} is a diagonal matrix with the eigenvalues of \mathbf{M}' ordered along the diagonal. Furthermore, in general $\vec{u}_i \cdot \vec{u}_j \neq 0$ and $\vec{u}_i^L \cdot \vec{u}_j^L \neq 0, \forall i, j$. However, $\vec{u}_i \cdot \vec{u}_i^L = 1$ and $\vec{u}_i \cdot \vec{u}_j^L = 0, \forall i \neq j$. Finally, as \mathbf{M}' is primitive as far as $0 < \mu < 2$, it follows that the highest eigenvalue and its associated eigenvector are positive, and $\lambda_1 > |\lambda_i|, \forall i > 1$. We will maintain the normalization $|\vec{u}_i| = 1$, which in general implies $|\vec{u}_i^L| \neq 1$.

The dependence with the selection parameter β acquired by the eigenvalues and eigenvectors of \mathbf{M}' preclude them from bearing any simple relation with the eigenvalues and eigenvectors of the adjacency matrix, contrary to what happened in the case of indistinguishable nodes. Still, the formal solution to the dynamics is similar to Eq. (5),

$$\vec{n}(t) = \mathbf{M}'^t \vec{n}(0) = \sum_{i=1}^m \lambda_i^t \alpha_i^L \vec{u}_i, \quad (29)$$

where α_i^L is the projection of the initial condition $\vec{n}(0)$ on the i th left eigenvector \vec{u}_i^L of \mathbf{M}' ,

$$\alpha_i^L = \vec{n}(0) \cdot \vec{u}_i^L. \quad (30)$$

The asymptotic state of the population is again given by \vec{u}_1 , which in this case corresponds to the right eigenvector associated to the largest eigenvalue λ_1 .

B. Formal results and relevant quantities

In the case of distinguishable nodes, it is not possible to obtain an explicit analytical dependence of the distance and the time to equilibrium as a function of μ and β , since topology and energy cannot be decoupled. Still, expressions analogous to Eqs. (13) and (14) are valid in this case. The distance $\Delta(t)$ to the equilibrium state can be written as

$$\Delta(t) \equiv \left| \frac{\mathbf{M}'^t \vec{n}(0)}{\lambda_1^t \alpha_1^L} - \vec{u}_1 \right| = \left| \sum_{i=2}^m \frac{\alpha_i^L}{\alpha_1^L} \left(\frac{\lambda_i}{\lambda_1} \right)^t \vec{u}_i \right|, \quad (31)$$

and the time to equilibrium is approximated to first order by

$$t_\epsilon^1 \simeq \frac{\ln|\alpha_2^L/\alpha_1^L| - \ln \epsilon}{\ln|\lambda_1/\lambda_2|}, \quad (32)$$

where, as before, we assume that the population has reached the equilibrium state when $\Delta(t) < \epsilon$, and $\epsilon < \epsilon_c$.

The introduction of the selection parameter β changes qualitatively the behavior of the system. Now there are two opposite forces: one tends to attract the population toward regions of maximal connectivity—or neutrality—(as shown in Sec. II B 1); the second does similarly toward regions of low energy—or high stability. The relative strength of these two selection pressures is tuned through β .

In the next two sections we are going to analyze the dynamics of the population as a function of the selection parameter β and the mutation rate μ , both during the transient toward equilibrium and at equilibrium. To this end we define two additional quantities, the *average energy* of the equilibrium distribution E and its *average dispersion* D . The *average energy* of the population $E(t)$ at time t is defined as

$$E(t) = \frac{\vec{E} \cdot \vec{n}(t)}{\sum_i n_i(t)}, \quad (33)$$

where \vec{E} is a vector whose element i is the energy corresponding to node i . When $t \rightarrow \infty$, we obtain the average energy of the equilibrium distribution,

$$E = E(t \rightarrow \infty) = \frac{\vec{E} \cdot \vec{u}_1}{\sum_i (u_1)_i}. \quad (34)$$

The *average dispersion* is a measure of how spread is the population on the network. We define it as the average over the minimum distance (in number of links, i.e. the minimum path) to go from node i to node j weighted by the corresponding populations. We thus define the distance matrix \mathbf{D} as the matrix whose element D_{ij} is the minimum path between nodes i and j . If i and j are connected $D_{ij}=1$, while the diagonal of \mathbf{D} fulfills $D_{ii}=0$. For a finite population of size $N(t)$, the average dispersion $D_N(t)$ at time t is

$$D_N(t) = \frac{\vec{n}(t) \mathbf{D} \vec{n}(t)^T N^2(t)}{\left(\sum_i n_i(t) \right)^2 N(t) (N(t) - 1)}, \quad (35)$$

where $\vec{n}(t)$ is the population as a row vector and $\vec{n}(t)^T$ is the population as a column vector. In the limit $N(t) \rightarrow \infty$ this expression becomes

$$D(t) = \frac{\vec{n}(t) \mathbf{D} \vec{n}(t)^T}{\left[\sum_i n_i(t) \right]^2}, \quad (36)$$

and when $t \rightarrow \infty$, we obtain the average dispersion at equilibrium,

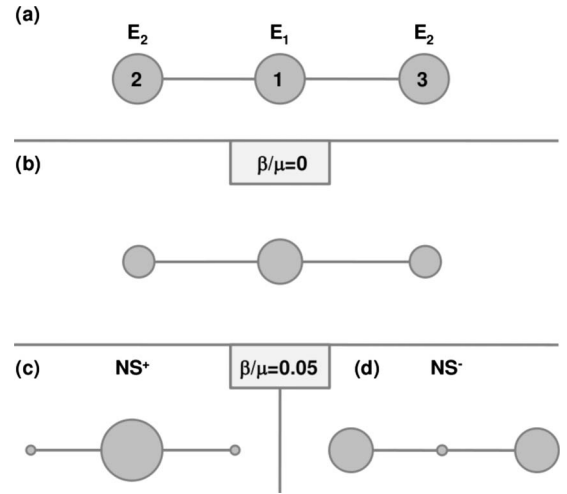


FIG. 2. (a) Schematic representation of the three-node network. In (b)–(d) the radius of the nodes is proportional to their occupancy at equilibrium. In (b), the ratio $\beta/\mu=0$ and the fraction of population in the central node is larger due to its higher degree ($k_1=2$). In (c) and (d), $\beta/\mu=0.05$, with positive correlation (NS^+ , $E_1=1$, $E_2=2$) in (c) and negative correlation (NS^- , $E_1=2$, $E_2=1$) in (d). $l=25$ in all cases. These two plots show the relevance of the degree-stability correlation in the final distribution of the population.

$$D = D(t \rightarrow \infty) = \frac{\vec{u}_1 \mathbf{D} \vec{u}_1^T}{\left(\sum_i (u_1)_i \right)^2}. \quad (37)$$

The minimum value of $D=0$ is attained when the population occupies a single node, while its maximum value, $D=D_M/2$ corresponds to half the population sitting at each of the two nodes for which $D_{ij}=D_M$ is maximum.

IV. EXACTLY SOLVABLE EXAMPLES OF NETWORKS WITH DISTINGUISHABLE NODES

In order to analyze the evolution of the populations with time or when the parameters are varied, we will pay special attention to four relevant quantities: the time t_ϵ that the population takes to reach the equilibrium state, [obtained from Eq. (31)], the average degree K of the population, Eq. (10); the average energy E , Eq. (34), and the average dispersion D , Eq. (37), the last three properties measured at equilibrium. Before attempting the numerical study of large, complex networks, to be presented in Sec. V, we analyze in this section two examples of networks with three and four nodes, since they allow full analytical treatment.

A. Three-node network

Consider the three-node network shown in Fig. 2(a), where one node with degree $k=2$ and folding energy E_1 is connected to two nodes of degree $k=1$ and folding energy E_2 . This is the simplest network containing nodes with different neutrality and energy. The matrix \mathbf{M}' is built following Eq. (27).

The corresponding eigenvalues are

$$\lambda_{1,3} = \frac{(2-\mu)(p_1+p_2)}{2} \pm \sqrt{\left(\frac{(2-\mu)(p_1-p_2)}{2}\right)^2 + 2p_1p_2\left(\frac{\mu}{3l}\right)^2}, \quad (38)$$

$$\lambda_2 = (2-\mu)p_2. \quad (39)$$

Since the second term under the square root above is much smaller than the first one, we can write

$$\lambda_{1,3} \approx (2-\mu)p_{\{1,2\}} \pm \frac{2p_1p_2}{|p_1-p_2|} \left(\frac{\mu}{3l}\right)^2, \quad (40)$$

where λ_1 always corresponds to the largest p_i in the first term on the right.

The right and left eigenvectors \vec{u}_i and \vec{u}_i^L associated read

$$\vec{u}_{1,3} = \frac{(-A \pm B, 1, 1)}{\sqrt{2 + (B \mp A)^2}}, \quad (41)$$

$$\vec{u}_{1,3}^L = \sqrt{2 + (B \mp A)^2} \frac{B \pm A}{4B} \left(\frac{2}{A \pm B}, 1, 1 \right), \quad (42)$$

$$\vec{u}_2 = \vec{u}_2^L = \frac{1}{\sqrt{2}}(0, -1, 1), \quad (43)$$

where $A = \frac{3(p_2-p_1)(2-\mu)l}{2p_2\mu}$, $B = \sqrt{A^2 + \frac{2p_1}{p_2}}$, $p_1 = \exp\{-\beta(E_1 - E_{min})\}$, and $p_2 = \exp\{-\beta(E_2 - E_{min})\}$.

As $\lambda_1 > \lambda_2 > \lambda_3$, $\forall E_1, E_2, l$, and $\mu > 0$, the eigenvector \vec{u}_1 obtained from Eq. (41) represents the equilibrium distribution for every set of parameters $(\beta, \mu, l, E_1, E_2)$.

1. Equilibrium properties

The explicit expressions obtained for eigenvalues and eigenvectors yield as well analytic solutions for the average energy E , the average degree K , and the average dispersion D . In what follows, we analyze the variation of these quantities with the stability parameter β and the mutation rate μ in two different regimes characterized by a different relationship between energy and degree of each node. Note that more energy means less stability, and vice versa:

(i) Regime NS^+ : neutrality and stability are positively correlated ($E_1 < E_2$).

(ii) Regime NS^- : neutrality and stability are negatively correlated ($E_1 > E_2$).

From Eq. (41), we can write the equilibrium distribution as $\vec{u}_1 = \frac{1}{\sqrt{((u_1)_1^*)^2 + 2}}((u_1)_1^*, 1, 1)$. Developing the term $(u_1)_1^*$ in series of β and μ (for $\beta < \mu$), we can obtain valuable information on how E , K , and D vary with the two parameters,

$$(u_1)_1^* \approx \sqrt{2} - \frac{3l}{2}(E_1 - E_2) \left(2 - \mu + \frac{\sqrt{2}\mu}{3l} \right) \frac{\beta}{\mu} + \frac{9l^2}{2\sqrt{2}}(E_2 - E_1)^2 \left(1 - \mu + \frac{\sqrt{2}\mu}{3l} \right) \frac{\beta^2}{\mu^2}, \quad (44)$$

plus terms of order $(\beta/\mu)^3$. Since the relevant range of mu-

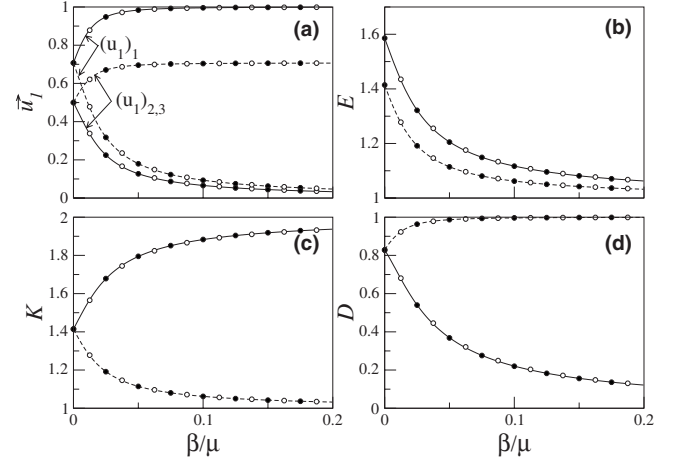


FIG. 3. Dependence of the equilibrium properties of the three-node network on β and μ for regimes NS^+ ($E_1 = E_{min} = 1$, $E_2 = 2$, solid line) and NS^- ($E_1 = 2$, $E_2 = E_{min} = 1$, dashed line). Each curve is plotted for $\mu = 0.001$ (\bullet), 0.01 (line) and 0.05 (\circ). The length of the sequence is $l = 25$. (a) Equilibrium distribution. Note that $(u_1)_2 = (u_1)_3$ for symmetry. (b) Average energy E . (c) Average degree K . (d) Average dispersion D .

tation rate values holds for $\mu \ll 1$, we can discard the terms proportional to μ added to terms of order one. Hence, the equilibrium state becomes a function of the ratio β/μ in a first approximation, $\vec{u}_1 \approx \vec{F}(\beta/\mu, l, E_1, E_2)$. As a consequence, and as far as μ is not too large, E , K and D also depend on β and μ through β/μ . We will see in Sec. V that this is a good approximation for much larger and more complex networks, giving a quantitative basis to the opposite and symmetric actions of β , enhancing selection of lower energy configurations, and μ , supporting evolution toward highly neutral states.

Figure 3 shows \vec{u}_1 , E , K , and D as a function of β/μ . The curves have been plotted varying β for three different values of μ , and all data collapse on the same curve, supporting the validity of approximating \vec{u}_1 and thus the quantities that depend on it as functions of the ratio β/μ . Furthermore, in Fig. 3(a) we see that in both regimes, NS^+ and NS^- , the equilibrium distribution is $\vec{u}_1 = 2^{-1}(\sqrt{2}, 1, 1)$ when $\beta/\mu = 0$ [see also Fig. 2(b) for a schematic], representing the case where energy does not affect the system ($\beta = 0$ and $p_1 = p_2 = 1$). However, when β/μ grows the results are highly dependent on the distribution of neutrality versus energy in the network. In regime NS^+ (that is, when the central node of degree $k=2$ has the lowest energy, $E_1 = 1$) if β/μ increases, the whole population moves toward the central node, as shown in Fig. 2(c). For this reason, we can observe in Fig. 3(b)–3(d) that, in this regime, E , K , and D asymptotically tend to the properties of node 1 when $\beta/\mu \rightarrow \infty$: $E \rightarrow E_1 = 1$, $K \rightarrow k_1 = 2$, and $D \rightarrow 0$. On the contrary, in the regime in which nodes 2 and 3 (with low neutrality, $k=1$) are more stable (NS^-), the population evolves toward these nodes, depleting the central node [see Fig. 2(d)]. The average energy, degree and dispersion of the population now tend to the values that they reach when the total population is equally distributed between nodes 2 and 3: $E \rightarrow E_2 = 1$, $K \rightarrow k_2 = k_3 = 1$, and $D \rightarrow 1$ when $\beta/\mu \rightarrow \infty$.

2. Time to equilibrium

As has been shown, the time t_ϵ^1 that a population takes to reach the equilibrium distribution starting from an initial condition $\vec{n}(0)$ [see Eq. (32)] approximates well the actual time to equilibrium t_ϵ [obtained from Eq. (31)] for small enough values of ϵ . In the following, working again in the approximation $\mu \ll 1$, we will derive the scaling form of t_ϵ^1 with the parameters β and μ for the three-node network. To this end, we define $t_\epsilon^1 = F_1 F_2$ and will develop to main orders in β and μ the two functions $F_1 = \ln|\alpha_2^t/\alpha_1^t| - \ln \epsilon$ and $F_2 = [\ln|\lambda_1/\lambda_2|]^{-1}$.

Let us write $\vec{u}_1^t = [(u_1^t)_1, (u_1^t)_2, (u_1^t)_3]$ and recall Eqs. (42) and (43). In this particular network, \vec{u}_2^t happens to be independent of β and μ . To make the calculation explicit, we consider as example the initial condition $\vec{n}(0) = (0, 1, 0)$ [42]. Hence, $\alpha_1^t = (u_1^t)_2$, and $\alpha_2^t = -1/\sqrt{2}$ is independent of β and μ (as \vec{u}_2^t also is). The only relevant term in the development of F_1 is $(u_1^t)_2$, for which the expression

$$(u_1^t)_2 \approx \frac{1}{2} - \frac{3l(\delta E)\beta}{4\sqrt{2}\mu} - \frac{9l^2(\delta E)^2\beta^2}{32\mu^2} + O\left(\frac{\beta}{\mu}\right)^3 \quad (45)$$

holds for $\beta < \mu$ and $\mu \ll 1$, with $\delta E = E_2 - E_1$. Substituting in the definition of F_1 and developing again,

$$F_1 \approx \ln\left(\frac{\sqrt{2}}{\epsilon}\right) + \frac{3\sqrt{2}l(\delta E)\beta}{4\mu} + \frac{9l^2(\delta E)^2\beta^2}{8\mu^2} + O\left(\frac{\beta}{\mu}\right)^3. \quad (46)$$

The function F_2 can be directly developed in powers of β and μ substituting Eqs. (38) and (39) in the definition of F_2 to obtain

$$F_2 \approx \left[\left(\frac{1}{2} - \frac{3l}{\sqrt{2}} \right) + \frac{1}{\mu} \left[3\sqrt{2}l - 9l^2(\delta E)\frac{\beta}{\mu} + \frac{27l^3(\delta E)^2\beta^2}{2\sqrt{2}\mu^2} + O\left(\frac{\beta}{\mu}\right)^3 \right] \right] \quad (47)$$

such that, finally,

$$t_\epsilon^1 \approx -\frac{3\sqrt{2}l-1}{4} \ln\left(\frac{2}{\epsilon^2}\right) + \frac{1}{\mu} \left[\frac{3l}{\sqrt{2}} \ln\left(\frac{2}{\epsilon^2}\right) + \frac{9(\delta E)l^2(2\ln \epsilon - \ln 2 + 1)\beta}{2\mu} + O\left(\frac{\beta}{\mu}\right)^2 \right] \quad (48)$$

The first term of t_ϵ^1 in Eq. (48) is negligible with respect to the second term. This implies that the resulting scaling form of the time to equilibrium is

$$t_\epsilon^1 \approx \frac{1}{\mu} F\left(\frac{\beta}{\mu}, l, E_1, E_2\right). \quad (49)$$

Figure 4 summarizes the dependence of different variables on the parameters β and μ . In all cases, we have used the initial condition $\vec{n}(0) = (0, 1, 0)$. Figures 4(a) and 4(b) show the variation in the eigenvalues λ_1 , λ_2 , and λ_3 of the transition matrix \mathbf{M}' as μ increases in the two regimes NS^+ and NS^- , respectively. As Eqs. (31) and (32) specify, the relation between the different eigenvalues is critical to deter-

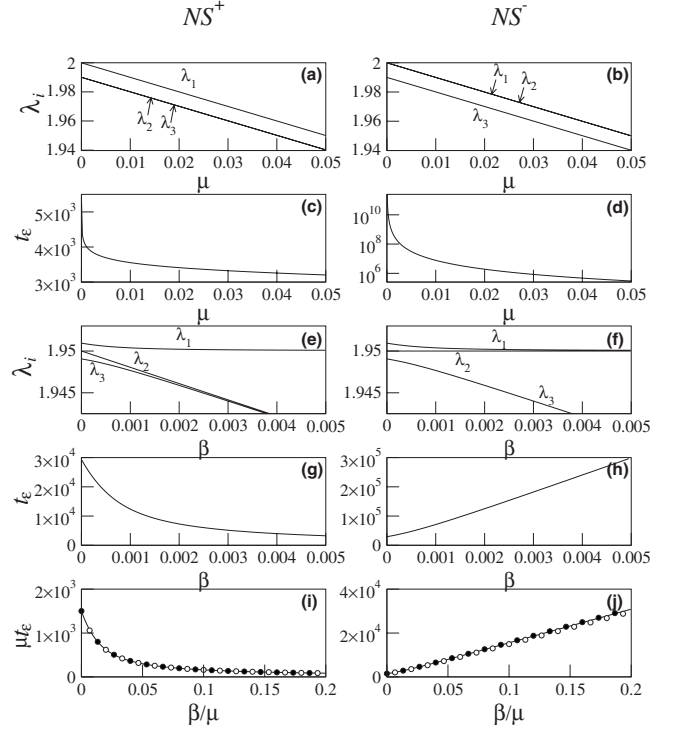


FIG. 4. Dependence of the eigenvalues of the transition matrix λ_i and the time to equilibrium t_ϵ of the three-node network on β and μ . The left-hand plots correspond to the NS^+ regime ($E_1 = E_{min} = 1$, $E_2 = 2$), while the right-hand plots correspond to the NS^- regime ($E_1 = 2$, $E_2 = E_{min} = 1$). The length of the sequence is $l = 25$. (a) and (b) λ_i when μ is varied, with $\beta = 0.005$. (c) and (d) t_ϵ when μ is varied and $\beta = 0.005$. (e) and (f) λ_i when β is varied and $\mu = 0.05$. (g) and (h) t_ϵ when β is varied and $\mu = 0.05$. (i) and (j) Dependence of μt_ϵ on β/μ . Each curve is plotted for $\mu = 0.001$ (●), 0.01 (solid line) and 0.05 (○). The corresponding value obtained with the approximation yielded by t_ϵ^1 is indistinguishable from the exact result up to the resolution of the figure.

mine the time required to reach the equilibrium distribution. In general, it is the ratio λ_1/λ_2 what determines whether this time will be long or short: if $\lambda_2 \rightarrow \lambda_1$, $t_\epsilon \rightarrow \infty$ while it is much smaller if $\lambda_2 \ll \lambda_1$. In Fig. 4(a), we see that $\lambda_1 \gg \lambda_2 \approx \lambda_3$. As (λ_1/λ_2) grows slowly with μ , the corresponding time to equilibrium, plotted in Fig. 4(c), will slowly decrease with μ . In Fig. 4(b), however, λ_2 has come close to λ_1 : $\lambda_1 = \lambda_2$ at $\mu = 0$, and their distance grows as μ^2 , see Eq. (40). As a consequence, when μ grows the time to equilibrium decreases, but as in this case $\lambda_1 \approx \lambda_2$, t_ϵ might reach comparatively high values [see Fig. 4(d)]. Figures 4(e) and 4(f) show the eigenvalues of the system when β is varied, while Fig. 4(g) and 4(h) depict the corresponding time to equilibrium. When β grows, λ_2 significantly differs from λ_1 in regime NS^+ , while $\lambda_1 = \lambda_2 + O(\mu^2)$ in regime NS^- . Therefore, β facilitates to reach equilibrium when neutrality and stability are positively correlated, but slows down the movement when they are negatively correlated. Finally, Figs. 4(i) and 4(j) show the relation between the rescaled times to equilibrium μt_ϵ and μt_ϵ^1 with β/μ for three values of μ and regimes NS^+ and NS^- , respectively. Numerical data approximately collapse on the same curve, which supports the scaling Eq.

(49). Furthermore, the accuracy of t_ϵ as compared to t_ϵ^1 in Eq. (31) in estimating the time to equilibrium is shown by the fact that both curves are indistinguishable up to the resolution of the figure.

In summary, when the mutation rate μ grows in a three-node network the time to equilibrium decreases monotonically, no matter what regime we are in. Furthermore, the time to equilibrium is several orders of magnitude higher in regime NS^- than in regime NS^+ . The reason is that in regime NS^- the population is obliged to spread on the network suffering two opposite forces: one pushes it toward the most connected region while the other one pushes it toward the most stable part of the network, and these two regions do not coincide. On the contrary, in regime NS^+ both pressures support the movement toward the same region of the network, making the evolution much faster.

B. Four-node network

Some properties of large networks, which are not observed in the three-node network due to its extreme simplicity, arise naturally in four-node networks. For this reason, we study in this section the network shown in Fig. 5(a), formed by one node with degree 3, two with degree 2, and one with degree 1. As it happened with the three-node system, the dynamics will strongly depend on the regime in which the network is. If neutrality and stability are positively correlated, the dynamics will be very similar to the three-node case in the same regime: the population will always tend to the most neutral region of the network, and increases in β will just enhance this tendency [see Figs. 5(b), 5(c), and 5(e)]. However, in regime NS^- the phenomenology shows an important new feature: for intermediate values of β/μ , the population might migrate to a region which represents a compromise between the two limit cases of maximum neutrality ($\beta/\mu \rightarrow 0$) and minimum energy ($\beta/\mu \rightarrow \infty$) [see Fig. 5(b), 5(d), and 5(f)].

Figure 6 summarizes the properties of the four-node network when neutrality and stability are negatively correlated. All quantities in Fig. 6(a), 6(b), and 6(d) can be calculated analytically, and are plotted for a wide range of β and three values of μ . The coincidence of the curves in (a) and (b) for different values of μ shows that the eigenvector \vec{u}_1 , and therefore E , K , and D , are functions of β/μ . The coincidence of the curves in (d) implies that $t_\epsilon \approx \frac{1}{\mu} F(\beta/\mu, l, E_1, E_2, E_4)$, as obtained for the three-node network. As \mathbf{M}' is a 4×4 matrix, these dependencies can be obtained explicitly, though the expressions are much more involved, and will not be presented here.

In Fig. 6(a) we can see the evolution with β/μ of the equilibrium distribution. Due to symmetry, $(u_1)_2 = (u_1)_3, \forall \mu, \beta$. When $\beta=0$ and the nodes are indistinguishable [see Fig. 5(b)], the population spreads searching for neutrality, and therefore most of it is in node 1 (where $k=3$), a little less in nodes 2 and 3 (where $k=2$), and very little population can be found in node 4 (where $k=1$). When β/μ increases, the population moves toward nodes 2 and 3 [see Fig. 5(d)], the average energy $E \rightarrow E_2 = E_3 = 2$, and the average degree $K \rightarrow k_2 = k_3 = 2$. Nodes 2 and 3 are less neutral and have lower

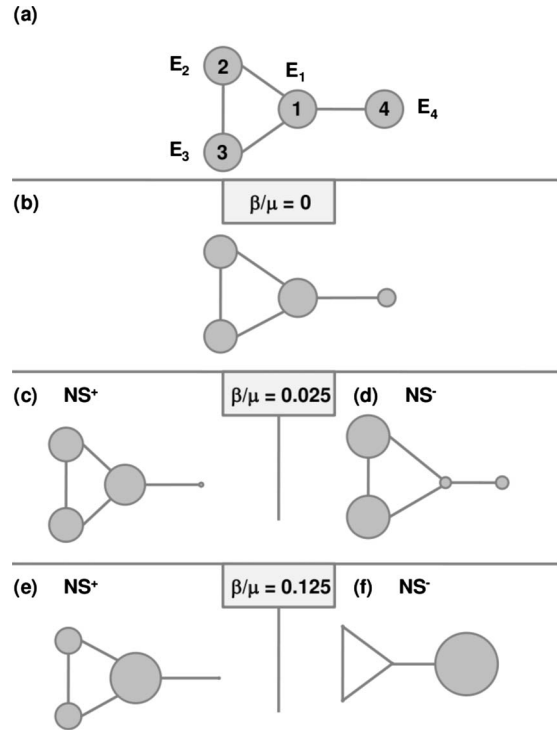


FIG. 5. (a) Schematic representation of the four-node network. In (b)–(f) the radius of the nodes is proportional to the size of the population in the equilibrium state. The parameters are $E_1 = E_{min} = 1.9, E_2 = E_3 = 2, E_4 = 4$ for the NS^+ regime, and $E_1 = 4, E_2 = E_3 = 2, E_4 = E_{min} = 1.9$, for the NS^- regime; $l = 25$. In the case of positive correlation (NS^+) the largest fraction of the population is always at the most connected node, and increases as β/μ grows [(b), (c) and (e)]. On the contrary, when the degree-stability correlation is negative (NS^-), the distribution of the population is very sensitive to the value of β/μ , which determines whether most of the population is located at the most connected node (b), is spread in an intermediate situation, (d) or occupies the most stable node (f).

energy than node 1, but are more neutral and have higher energy than node 4, therefore behaving as an intermediate situation between the initial search for neutrality and the final migration toward the region of lowest energy in the network. When β/μ is increased slightly further, the population keeps on filling nodes 2 and 3, beginning simultaneously to occupy node 4, located in the opposite side of the graph. In fact, there is a critical value $(\beta/\mu)_B \approx 0.075$ for which all stable nodes (2, 3, and 4) are very populated, while that with the highest connectivity (node 1) is almost empty. This is clearly signaled with a maximum in the time to equilibrium and in the average dispersion. When β/μ crosses the critical point [marked with B in Fig. 6(c) and 6(d)] the population finally migrates toward node 4 [see Fig. 5(f)], which is the most energetically stable. When $\beta/\mu \rightarrow \infty$, the equilibrium properties of the population tend to their asymptotic values $E \rightarrow E_4 = 1.9, K \rightarrow k_4 = 1$ and $D \rightarrow 0$.

Figure 6(c) shows the dependence of the eigenvalues λ_i with the stability parameter β , for $\mu = 0.05$ (they are represented against β/μ just to compare with the other plots). In the three-node system, t_ϵ varied monotonically with μ for all regimes, increased with increasing β in the NS^+ regime and

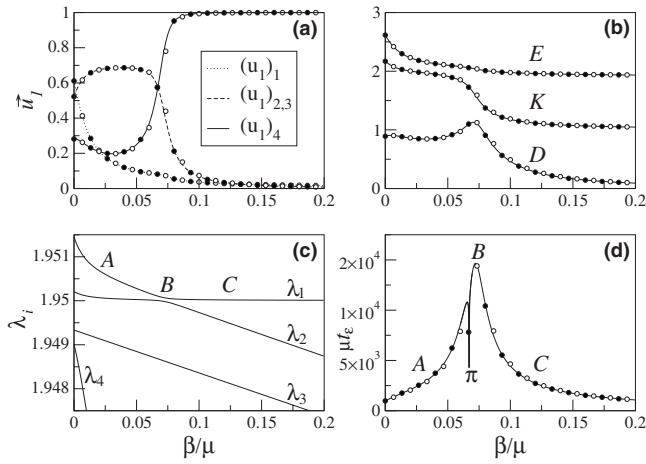


FIG. 6. Dependence of the properties of the four-node network on β and μ when neutrality and stability are negatively correlated. The parameters are as in Fig. 5. Each curve is plotted for $\mu = 0.001$ (\bullet), 0.01 (line) and 0.05 (\circ) in (a), (b), and (d). (a) Equilibrium distribution. (b) Equilibrium properties: average energy E , average degree K and average dispersion D . (c) Eigenvalues λ_1 , λ_2 , λ_3 , and λ_4 for $\mu = 0.05$. (d) Dependence of μt_ϵ on β/μ .

vice versa in the NS^- regime. In the four-node system, in the NS^+ regime the relation λ_1/λ_2 (which dominates t_ϵ for most values of the parameters) also grows monotonically in most cases with μ and β . Therefore, t_ϵ generically decreases when any of these two parameters grow. However, in the NS^- regime (the case plotted in Fig. 6), the two largest eigenvalues λ_1 and λ_2 approach each other when $\beta/\mu < (\beta/\mu)_B$ and move apart when $\beta/\mu > (\beta/\mu)_B$. They do not cross, however, as demonstrated by the Perron-Frobenius theorem (see Sec. III). The rescaled time to equilibrium, plotted in Fig. 6(d), shows a maximum when the difference between the two eigenvalues becomes minimum.

In Fig. 6(d) we have plotted t_ϵ and t_ϵ^1 in the same plot. As it happened in the three-node network, both quantities are indistinguishable up to the resolution of the figure. Furthermore, the effect of the initial condition $\vec{n}(0)$ in t_ϵ is especially relevant in certain parameter range. This is the case of values of μ and β for which $|\alpha_2^t| = |\vec{n}(0)\vec{u}_2^t| \ll |\alpha_1^t| = |\vec{n}(0)\vec{u}_1^t|$, causing the term $\ln|\alpha_2^t/\alpha_1^t|$ in Eq. (32) become of the order of $\ln(\epsilon)$. In Fig. 6(d), this effect is especially important around $\beta/\mu \approx 0.068$ (π in the plot), for which $\alpha_2^t \approx 0$, thus producing a severe minimum in the time to equilibrium.

Finally, Fig. 7 shows the evolution of eigenvectors \vec{u}_1 and \vec{u}_2 in the vicinity of the critical point B [points A , B , and C are also marked in Figs. 6(c) and 6(d)]. Both eigenvectors have been projected over the two first eigenvectors in region A , \vec{u}_{1A} , and \vec{u}_{2A} , corresponding to the value $\beta/\mu = 0.035$. The vertical axis thus represents the scalar product $\vec{u}_i \cdot \vec{u}_{jA}$, for $i, j = 1, 2$. As \vec{u}_1 and \vec{u}_2 go through the critical value $\beta/\mu \approx 0.075$, they seem to exchange gradually their roles (but note that \vec{u}_1 is a positive vector, while \vec{u}_2 is not). As a direct consequence, near B the population spreads over a significantly large region of the network that contains the populated nodes in region A and in region C , thus resulting in a maximum for the average dispersion of the population D at B . In summary, the mutual influence between eigenvalues and

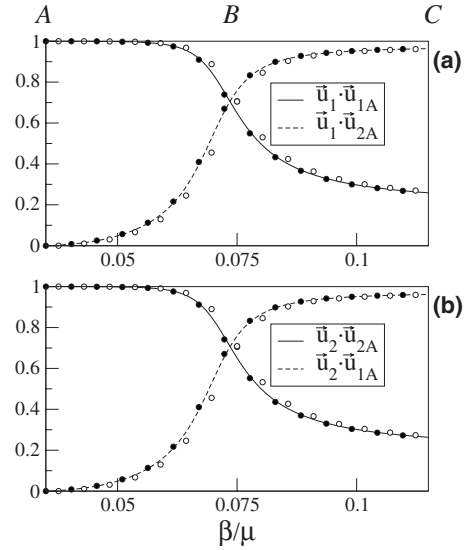


FIG. 7. Evolution of eigenvectors \vec{u}_1 and \vec{u}_2 in the vicinity of the critical point B . Each curve is plotted for $\mu = 0.001$ (\bullet), 0.01 (line) and 0.05 (\circ). (a) Projection of \vec{u}_1 on \vec{u}_{1A} and \vec{u}_{2A} [where $(\beta/\mu)_A = 0.035$]. (b) Projection of \vec{u}_2 on \vec{u}_{1A} and \vec{u}_{2A} .

eigenvectors is the key to understand the migrations that a population might suffer when the system parameters are varied.

V. COMPLEX NETWORKS

The goal of this section is to extend our results to more complex networks, in order to show the generality of the dynamics and methods discussed in previous sections. Two different kinds of test networks are presented and analyzed: the *random mutation* network and the *preferential mutation* network. Each node will be now explicitly represented by a sequence whose energy will depend on its composition. The links in each network respect the basic rules underlying natural RNA neutral networks.

A. Network construction

Random mutation (RM) and preferential mutation (PM) networks are constructed starting with a genomic sequence of length l . New sequences (nodes) are progressively added in such a way that the growing network is always connected.

In the RM network, each sequence in the network has probability $q = 1/M(\tau)$ to be chosen at step τ to generate a new sequence through a single mutation, being $M(\tau)$ the number of nodes at step τ . Initially, $M(1) = 1$ and the seed sequence is thus chosen with probability $q = 1$. One of the nucleotides in the selected sequence, randomly chosen, is then mutated and the two sequences are linked. Further, the new sequence is linked to any other sequence in the network which is at a Hamming distance of one. The procedure is repeated until $\tau = m$, thus generating a connected network with $M(m) = m$ nodes.

The expected degree $\langle k_i \rangle$ of the sequence introduced at step τ is

$$\langle k_\tau \rangle = 1 + \sum_{i=\tau+1}^{m-1} \frac{1}{i}, \quad (50)$$

where, in a first approximation, we have discarded the links due to sequences at a Hamming distance of one different from the mother sequence of the new node. This expression works well for $l \gg 1$ and $m \ll 4^l$, a regime where networks are diluted and the number of triangles is small. In the regime where $m > \tau \gg 1$, we can substitute the sum by an integral to obtain $\langle k_\tau \rangle \approx 1 + \ln(m-1) - \ln(\tau+1)$. This function is actually a Zipf ordering of the degree k of the nodes as a function of their rank (which, in turn, is equal to the step of insertion in the network τ). The inverse function $\tau(k)$ stands for the number of nodes with degree larger than k . Hence, if we define $m_k = mP_{RM}(k)$ as the number of nodes with degree k —where $P_{RM}(k)$ is the probability density distribution of the degree—, the relation

$$\tau(k) = \int_k^\infty P_{RM}(k') dk' \quad (51)$$

holds for $m > \tau \gg 1$. Within this approximation, and by virtue of Eq. (51), the maximum degree expected is $k_{max} \approx \ln m$.

Finally, we obtain that the degree distribution decays as

$$P_{RM}(k) \approx e^{-k}. \quad (52)$$

A different derivation of this result has been presented in previous publications studying networks growing through a random attachment model in a mean-field approximation [31–33]. It was shown that the average number $\langle c \rangle$ of links per added node changes the slope of the exponential distribution, such that $P_{RM}(k) \propto e^{-k/\langle c \rangle}$. In our model, relatively small values of l lead to the introduction of additional links to those sequences at a Hamming distance of one, thus modifying quantitatively (not qualitatively) the exponential degree distribution derived.

The algorithm used to construct the PM network is inspired in the Barabási-Albert (BA) preferential attachment model of network growth [34]. The BA model successfully describes the heterogeneity in the degree distribution of many biological, technological and social networks [35,36]. These networks are characterized by a degree distribution that follows a power law, and by the presence of highly connected nodes, known as hubs. In our case, the network growth process is similar to the one proposed for the RM networks, but in this case the probability q that a node i is selected to mutate and thus generate a new node in the network depends on the degree k_i of the node and varies with the step: $q = k_i / \sum_i k_i$, for $i = 1, \dots, M(\tau)$. As expected, the PM networks obtained with the BA model are characterized by the existence of hubs and a truncated power-law decay in their degree distributions, the latter due to the fact that in neutral networks the highest degree has an upper bound of $3l$, being l the length of the sequence. The expected degree distribution is given by the preferential attachment BA model,

$$P_{PM}(k) \approx Ck^{-3}, \quad (53)$$

where the maximum degree expected grows as $k_{max} \propto m^{1/3}$ (for $4^l \gg m \gg (3l)^3$ and $k_{max} \leq 3l$). Within the approximation $l \gg 1$ and $m \ll 4^l$, the correction due to links caused by pre-existing sequences at Hamming distance of one (different from the mother sequence) is small and does not affect the functional form above, only modifying the proportionality coefficient C .

Despite the deviations from the predicted maximum degree and from the distributions $P_{RM}(k)$ and $P_{PM}(k)$ expected for small m and finite l , the quantities derived above serve to illustrate the topological differences in networks constructed following one or another algorithm [31–33]. These differences have a remarkable effect in the dynamics of the population, as will be shown in the next section.

The energy associated to each sequence in the network will be now defined as a function of its composition. It is well known that the minimum free energy of an RNA secondary structure depends on the nucleotidic composition of the sequence folding into it [25,26]. Approximately, pairs G-C decrease the energy of an open structure in 3 kcal/mol, A-U pairs in 2 kcal/mol and G-U pairs in 1 kcal/mol. For sequences belonging to the neutral networks computationally generated, we define the energy of a node as

$$E_i = -(3N_{GC} + 2N_{AU} + N_{GU}), \quad (54)$$

where N_{GC} and N_{AU} are independent quantities corresponding to the maximum number of pairs G-C or A-U that can be formed with the current sequence. They correspond to $\text{Min}\{\#G, \#C\}$ and $\text{Min}\{\#A, \#U\}$. In case of an excess of both G and U, pairs G-U would be formed. For example, the sequence $s = \text{AAUGCACUCAAGGG}$ has energy $E_s = -13$ kcal/mol: it can form three pairs G-C, two pairs A-U, and there is no excess of U to pair with the G in excess. Note that with this simple definition we do not take into account geometrical constraints. Actually, the energy of a folded sequence defined as in Eq. (54) is a lower bound to the energy obtained by realistic folding algorithms. An absolute lower bound to the energy of a sequence of length l is $E_{min} = -3l/2$ when l is an even number and $E_{min} = -3(l-1)/2$ when l is an odd number. With this definition of energy we consider in a natural fashion the relatively smooth variation in the energy of neighboring sequences (whose composition varies smoothly by construction) in the network.

We can control as well the correlation between degree and energy. Networks whose construction started from an initial node with a sequence made of GC repeats represent the NS^+ regime, since this sequence has the minimum possible energy $E_{(GC)^{l/2}} = E_{min} = -36$ kcal/mol and the initial nodes will be those of higher degree, as has been shown. On the other hand, networks that begin with a poly-A sequence (i.e., AAAA...) resemble the NS^- regime because the energy associated to this sequence, unable to form any base pair, is the maximum possible: $E_{(A)^l} = 0$ kcal/mol.

B. Population dynamics

In the numerical simulations discussed in this section, we have constructed two networks following the algorithms RM

TABLE I. Summary of the main network parameters: number of nodes m , number of links \mathcal{M} , mean degree $\langle k \rangle$, largest degree k_{max} , mean geodesic path L between all nodes of the network, diameter L_{max} (longest distance between any pair of nodes), global clustering coefficient C (fraction of triangles) and highest eigenvalue γ_1 of the adjacency matrix.

	RM Network	PM Network
m	200	200
\mathcal{M}	218	250
$\langle k \rangle$	2.18	2.50
k_{max}	11	25
L	8.41	5.26
L_{max}	20	10
C	0.0767	0.1100
γ_1	4.099	6.035

and PM previously described with $l=25$ and $m=200$. Table I summarizes the main topological parameters in either case. Apparently, both networks have properties reminiscent of small-world networks [37], i.e., a low mean geodesic distance L between all nodes and a high clustering coefficient C (see Table I caption for details). However, in our case, the small-world topology is not caused by the presence of true shortcuts, but results from the high dimensionality of the genome space. In addition, note that the minimum path between two sequences differing in nt nucleotides is at least nt , thus revealing the underlying regular network. We can directly appreciate an excess in the number of links caused by the presence of sequences in the network at a Hamming distance of one different from the mother sequence: in the limit $l \rightarrow \infty$, the expected number of links in a network of m nodes constructed through either algorithm is $\mathcal{M}_{l \rightarrow \infty}(m) \approx m$.

The main properties of the evolution on the RM and PM networks in the NS^+ regime, that is, when stability and degree are positively correlated, are very similar to those obtained in the three-node and the four-node networks. For $\beta/\mu=0$, we have seen that the topology of the network fully determines the evolution of the population. As β/μ grows, the population is increasingly attracted to the most stable region from the energetic viewpoint which, in turn, is the most connected one. This positive feedback leads to a smooth contraction of the population around the most stable and connected node. As a consequence, the time to equilibrium shows, once more, very low values.

On the contrary, when the population evolves on a network in the NS^- regime, i.e., when stability and degree are negatively correlated, the phenomenology gets richer. Figure 8 shows the main properties of the RM network analyzed in Table I as a function of β/μ in the NS^- regime, and Fig. 9 shows the same quantities for the PM network. The equilibrium properties E , K , and D are shown in plots (a), (b), and (c), respectively, while (d) displays for both figures the rescaled times to equilibrium μt_ϵ and μt_ϵ^1 . All quantities have been calculated for $\mu=0.001, 0.01$, and 0.05 , and they all collapse on the same curve. This agreement suggests that the dependence of \bar{u}_1 (and therefore E , K , D), and μt_ϵ on β/μ

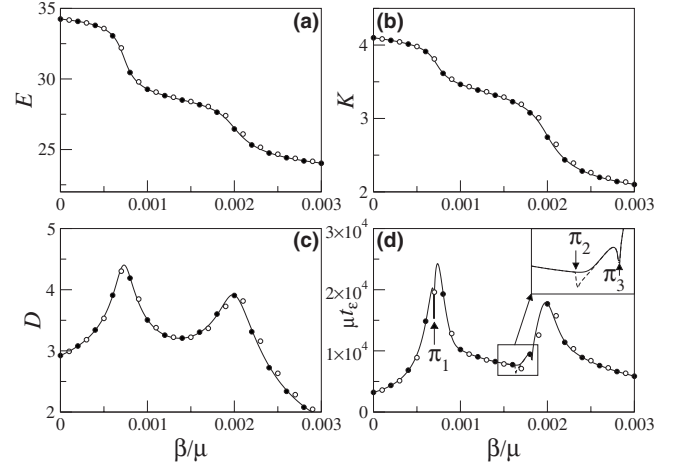


FIG. 8. Dependence of the properties of the random mutation (RM) network on β and μ when neutrality and energetic stability are negatively correlated (NS^-). Each curve is plotted for $\mu = 0.001$ (\bullet), 0.01 (solid line), and 0.05 (\circ). (a) Average energy E . (b) Average degree K . (c) Average dispersion D . (d) Dependence of the rescaled time to equilibrium with β/μ . The solid line stands for t_ϵ [obtained from Eq. (31)], and the dashed line represents t_ϵ^1 [Eq. (32)].

that we could analytically prove for the three-node and the four-node networks can be generalized to networks of arbitrary size and topology.

When comparing both networks, we see that the transition from the most connected area to the lowest energy nodes is relatively smooth in the RM network and very abrupt in the PM network. In the case of RM networks, where the degree distribution is more uniform than in the PM case, the possibility of multiple migrations is higher and transitions are thus more gradual for the same parameters. This fact is reflected in Fig. 8, where the equilibrium properties E and K apparently show three broad plateaus as β/μ grows. Furthermore, the maxima of the average dispersion D and the time to equilibrium t_ϵ , that typically coincide with the migrations, show relatively flat peaks. On the contrary, in the PM net-

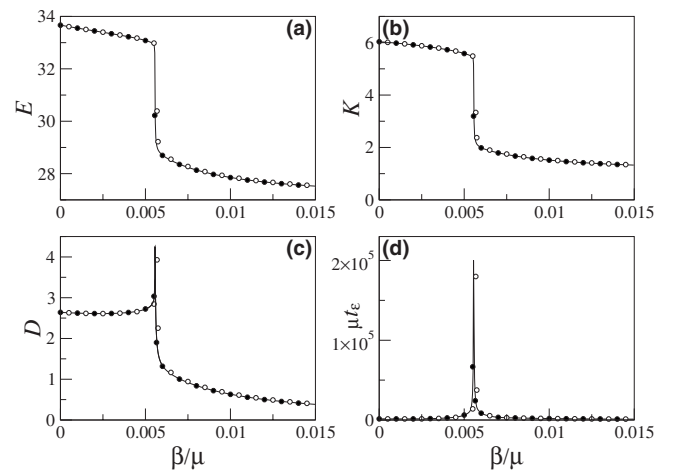


FIG. 9. Same as in Fig. 8 for the preferential mutation (PM) network. In plot (d), t_ϵ and t_ϵ^1 are indistinguishable up to the resolution of the figure.

work the dynamics of the population is mainly characterized by the existence of a unique node of degree 25. This hub strongly attracts the population, until the influence of the most stable node is so intense that a sudden migration occurs. As a direct consequence, the maxima of the average dispersion D and the time to equilibrium t_ϵ are remarkably sharper in this case.

The dynamic behavior of the population on the RM and PM networks is mainly controlled by the largest eigenvalues of the transition matrix. We know that λ_1 is a nondegenerate eigenvalue (see Sec. III) and, though we do not have a mathematical proof for other eigenvalues, our numerical studies indicate that they do neither cross (i.e., $\lambda_i > \lambda_{i+1} \forall i, \beta, \mu$) in large, heterogeneous networks. However, as β/μ changes, consecutive eigenvalues can get very close one to another and exchange their associated eigenvectors, causing qualitative changes in the average energy, the time to equilibrium, and other macroscopic variables. This complex situation might produce a number of maxima in t_ϵ , for instance, that depends on the precise topology and energy distribution of each network.

As we have already seen throughout the paper, the time to equilibrium is also influenced by the initial condition $\vec{n}(0)$. For certain values of β/μ , it may happen that $|\alpha_2^t| \ll |\alpha_1^t|$, causing the time to equilibrium to be especially short [see Eq. (32), and Sec. IV B for the analogous phenomenon in the four-node network]. In Fig. 8(d) this happens for three values of β/μ , signaled with arrows in π_1 , π_2 , and π_3 . The time to equilibrium t_ϵ is plotted as a solid line, while t_ϵ^1 [Eq. (32)] is plotted as a dashed line. This approximation is usually very good, but as we discussed in Secs. II and III, if the influence of the higher-order eigenvalues is not negligible, Eq. (32) does not yield accurate enough results. The only region of the figure where t_ϵ and t_ϵ^1 do not coincide (to the resolution of the plot) is around π_2 , a region enlarged in Fig. 8(d) for clarity. In the small region around π_2 , it happens that $|\alpha_3^t| \gg |\alpha_2^t|$, and λ_3 is so close to λ_2 that the approach to equilibrium is ruled by the third eigenvalue λ_3 : as a result, the minimum expected by Eq. (32) in π_2 vanishes and does not appear in an exact computation.

Finally, Figs. 10 and 11 show two examples of the equilibrium distribution of the population on the RM and the PM network, respectively, for the NS^- regime and representative values of β/μ . In the RM case, the plots correspond to the three plateaus observed in Fig. 8; in the PM case, the pictures show one situation below the critical value of β/μ and one above it. As we already mentioned, the lack of very large hubs in the RM network gives rise to smooth transitions and allows two different migrations as β/μ grows. On the contrary, in the PM network the dynamics of the population is mainly characterized by the existence of a unique but very strong hub, that allows the existence of only two regimes when β/μ is varied. Consequently, the migration toward the most stable node, which in fact has degree one, is certainly abrupt.

VI. CONCLUSIONS

The evolution of a population of replicators on networks of selectively neutral genotypes depends on the topology of

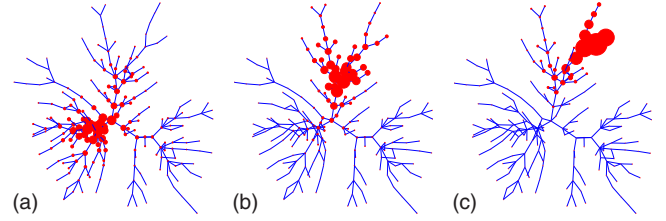


FIG. 10. (Color online) Final distribution of the population in the NS^- regime for the RM network. The area of each node is proportional to its population. (a) $\beta/\mu=0.0005$. The selection of low energy is weak and the population stays around the most connected area. (b) $\beta/\mu=0.0014$. The population escapes from the most connected region and, in its movement toward the most stable node, it stacks into an area of moderate neutrality and low energy. (c) $\beta/\mu=0.0027$. Stability overcomes neutrality and the population is located around the most stable node. See Fig. 8 to obtain the values of E , K , and D in each situation.

the network and on the mutation rate μ , which determines the time to equilibrium. When exact neutrality is broken through the introduction of an energy for the nodes, two competing selection pressures (toward highly neutral configurations or toward low-energy states) lead to different equilibrium states. The time to equilibrium becomes then a complex function of μ and the selection parameter β . Our analyses of small networks have shown that relevant equilibrium properties as the average energy of the population, the average degree, or the average dispersion on the network, are functions of the rescaled parameter β/μ : β pushes the population toward the most stable regions of the network, while μ promotes neutrality and generically diminishes the time to equilibrium.

In the cases studied, we have seen how relevant the correlation between energy and degree is by extending the study to complex networks in different regimes. Remarkably, the phenomenological behavior in such networks is qualitatively identical to what has been observed in simpler networks: for positive degree-stability correlations (NS^+), where the most neutral regions are also the most stable ones, the evolution of the population is smooth as β/μ increases. On the other hand, sudden migrations are observed when neutrality and stability are negatively correlated (NS^-). This occurs when

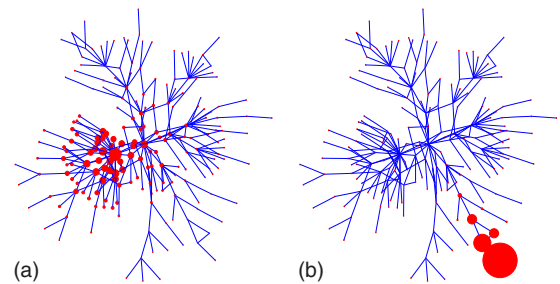


FIG. 11. (Color online) Same as Fig. 10 for the PM network. (a) $\beta/\mu=0.0025$. The energy dependence is not enough to overcome the high neutrality of the most connected nodes. (b) $\beta/\mu=0.01$. The critical value $\beta/\mu \approx 0.0055$ has been crossed and the population has drifted toward the most stable node (bottom-right node of the figure). See Fig. 9 to obtain the values of E , K , and D in each situation.

the eigenvalues λ_1 and λ_2 get very close. In addition, the influence of the initial condition can be relevant in accelerating the process and, occasionally, eigenvalues of higher order can induce more complex dynamics in a way that we have quantified.

Our study has been motivated by current knowledge of networks of selectively neutral genotypes (notably RNA secondary structure neutral networks), and in particular by the prediction that the degree of neutrality of a population increases through evolution. However, highly neutral genotypes are rarely observed in nature. We have shown that the time to achieve the region of high neutrality is larger the smaller is the mutation rate, and depends in a nontrivial (case-dependent) manner on the size and topology of the network. In future studies, it would be interesting to compare the typical time scale μ^{-1} with the typical time during which an environment keeps constant to determine to what extent is high neutrality an observable property of such systems. The introduction of a second selection pressure uncorrelated to neutrality might cause major deviations from highly neutral states, and prevents its achievement in generic situations. At present, the astronomically large sizes of neutral networks of RNA sequences forbid systematic studies on such networks.

Previous studies have shown that neutral networks of RNA secondary structures display a substantial correlation between the degree of a sequence and the energy of the corresponding minimum free-energy folded configuration [38]

(in a way that would be represented by the NS^+ regime in this paper). In principle, thus, the dynamics of RNA populations is canalized toward more stable and more neutral states. In simple models of heteropolymer folding, the assumption of a positive correlation between neutrality and stability (our NS^+ regime) originates funnels in sequence space that direct the population toward sequences with high neutrality and high stability [16]. This, however, does not preclude that, in cases where other features optimized in different regions of the genome space happen to be under strong selection (an example could be specific sequences characterizing active molecular sites), also populations of RNA sequences, heteropolymers, or proteins, could show sudden migrations toward regions that better fulfill all simultaneous adaptive requirements. The implications of the dynamics we have characterized in the evolution of populations of replicators under changing environments (requiring different phenotypes and thus competence between different neutral networks) will be a subject of future research.

ACKNOWLEDGMENTS

The authors gratefully acknowledge enlightening discussions with Juan A. Almendral, José A. Cuesta, Daniel Peralta-Salas, and Michael Stich, and the support of Spanish MICIIN through Project No. FIS05273-2008.

-
- [1] M. Kimura, *Nature (London)* **217**, 624 (1968).
 [2] L. W. Ance and W. Fontana, *J. Exp. Zool.* **288**, 242 (2000).
 [3] W. Fontana, *BioEssays* **24**, 1164 (2002).
 [4] P. Schuster, *Rep. Prog. Phys.* **69**, 1419 (2006).
 [5] P. Schuster, W. Fontana, P. F. Stadler, and I. L. Hofacker, *Proc. R. Soc. B* **255**, 279 (1994).
 [6] P. C. Anderson and S. Mecozi, *J. Am. Chem. Soc.* **127**, 5290 (2005).
 [7] M. Eigen, *Naturwiss.* **58**, 465 (1971).
 [8] J. J. Holland, J. C. de la Torre, and D. A. Steinhauer, *Curr. Top. Microbiol. Immunol.* **176**, 1 (1992).
 [9] C. Briones, M. Stich, and S. C. Manrubia, *RNA* **15**, 743 (2009).
 [10] C. Reidys, P. F. Stadler, and P. Schuster, *Bull. Math. Biol.* **59**, 339 (1997).
 [11] E. A. Schultes and D. P. Bartel, *Science* **289**, 448 (2000).
 [12] K. Koelle, S. Cobey, B. Grenfell, and M. Pascual, *Science* **314**, 1898 (2006).
 [13] C. V. Forst, C. Reidys, and J. Weber, in *Advances in Artificial Life, 929 of Lecture Notes in Artificial Intelligence*, edited by F. Morán, A. Moreno, J. J. Merelo, and P. Chacón, (Springer, Berlin, 1995), p. 128.
 [14] C. Reidys, C. V. Forst, and P. Schuster, *Bull. Math. Biol.* **63**, 57 (2001).
 [15] E. van Nimwegen, J. P. Crutchfield, and M. Huynen, *Proc. Natl. Acad. Sci. U.S.A.* **96**, 9716 (1999).
 [16] E. Bornberg-Bauer and H. S. Chan, *Proc. Natl. Acad. Sci. U.S.A.* **96**, 10689 (1999).
 [17] Sumedha, O. C. Martin, and L. Peliti, *J. Stat. Mech.* 2007, P05011.
 [18] R. Forster, C. Adami, and C. O. Wilke, *J. Theor. Biol.* **243**, 181 (2006).
 [19] C. O. Wilke, *Bull. Math. Biol.* **63**, 715 (2001).
 [20] C. O. Wilke, *Evolution* **55**, 2412 (2001).
 [21] E. Borenstein and E. Ruppin, *Proc. Natl. Acad. Sci. U.S.A.* **103**, 6593 (2006).
 [22] F. M. Codoñer, J. A. Daros, R. V. Solé, and S. F. Elena, *PLoS Pathog.* **2**, e136 (2006).
 [23] R. E. Lenski, J. E. Barrick, and C. Ofria, *PLoS Biol.* **4**, e428 (2006).
 [24] J. Aguirre, E. Lázaro, and S. C. Manrubia, *J. Theor. Biol.* **261**, 148 (2009).
 [25] C. Workman and A. Krogh, *Nucleic Acids Res.* **27**, 4816 (1999).
 [26] J. C. Biro, *Theor. Biol. Med. Model.* **5**, 14 (2008).
 [27] F. R. Gantmacher, *The Theory of Matrices* (Chelsea, New York, 1960), Vols. I and II.
 [28] H. Minc and M. Marcus, *A Survey of Matrix Theory and Matrix Inequalities* (Prindle, Weber and Schmidt, Toronto, 1964).
 [29] *Handbook of Graph Theory*, edited by J. L. Gross and J. Yellen (CRC Press, New York, 2004).
 [30] J. J. Bull, L. A. Meyers, and L. Lachmann, *PLoS Comput. Biol.* **1**, e61 (2005).
 [31] A.-L. Barabási, R. Albert, and H. Jeong, *Physica A* **272**, 173 (1999).
 [32] P. L. Krapivsky and S. Redner, *Phys. Rev. E* **63**, 066123

- (2001).
- [33] S. N. Dorogovtsev and J. F. F. Mendes, *Adv. Phys.* **51**, 1079 (2002).
- [34] A.-L. Barabási and R. Albert, *Science* **286**, 509 (1999).
- [35] M. E. J. Newman, *SIAM Rev.* **45**, 167 (2003).
- [36] S. Boccaletti, V. Latora, Y. Moreno, M. Chavez, and D.-U. Hwang, *Phys. Rep.* **424**, 175 (2006).
- [37] D. J. Watts and S. H. Strogatz, *Nature (London)* **393**, 440 (1998).
- [38] S. Wuchty, W. Fontana, I. L. Hofacker, and P. Schuster, *Biopolymers* **49**, 145 (1999).
- [39] A matrix is irreducible when the corresponding graph is connected; in our case any pair of nodes i and j of the network are connected via mutations by definition. Irreducibility plus the condition $M_{ii} > 0, \forall i$ makes matrix \mathbf{M} primitive. See [27–29] for further details on matrix theory and spectral graph theory.
- [40] In order to calculate the evolution of the population to equilibrium we cannot choose an homogeneous distribution for a completely connected graph, since this initial condition is proportional to the equilibrium distribution. The initial condition $\vec{n}(0) = (1, 0, 0, \dots, 0)$ applied to the star graph does not modify the reported dependence with m .
- [41] Two square matrices \mathbf{A} and \mathbf{B} are called similar if $\mathbf{A} = \mathbf{N}^{-1}\mathbf{B}\mathbf{N}$ for some invertible matrix \mathbf{N} . Similar matrices share many properties, such as the eigenvalues (but not the eigenvectors) and the fact that, if one is diagonalizable, the other is also diagonalizable. Applying this definition, $\mathbf{M}' = \mathbf{E}\mathbf{M}$ is similar to the symmetric matrix $\mathbf{E}^{1/2}\mathbf{M}\mathbf{E}^{1/2}$, because $\mathbf{E}^{1/2}$ is invertible [it is diagonal and $(E^{1/2})_{ii} > 0, \forall i$]. This means that the eigenvalues λ_i of \mathbf{M}' are real and the matrix diagonalizable, allowing the decomposition shown in Eq. (28).
- [42] It is important to mention that the highly symmetric configuration of this network forbids to use an homogeneous initial condition $\vec{n}(0) = \frac{1}{\sqrt{3}}(1, 1, 1)$ if we wish to use the approximation t_ϵ^1 , since it yields $\alpha_2 = 0, \forall \mu$ and β , and thus violates the conditions of applicability of the first-order approximation to the time to equilibrium. The actual time to equilibrium t_ϵ is in that particular case dominated by the ratio λ_1/λ_3 .